Received: 5 November 2020 | Revised: 15 January 2021 | Accepted: 14 February 2021

DOI: 10.1002/humu.24186

RESEARCH ARTICLE

Human Mutation HGVS HUMAN GENOME VARIATION SOCIETY WILEY

A global analysis of the reconstitution of PTEN function by translational readthrough of *PTEN* pathogenic premature termination codons

Sandra Luna[1] | Leire Torices[1] | Janire Mingo[1] | Laura Amo[1] | Isabel Rodríguez-Escudero[2] | Pablo Ruiz-Ibarlucea[1] | Asier Erramuzpe[1] | Jesús M. Cortés[1,3] | María I. Tejada[1] | María Molina[2] | Caroline E. Nunes-Xavier[1,4] | José I. López[1,5] | Víctor J. Cid[2] | Rafael Pulido[1,3]

[1]Biocruces Bizkaia Health Research Institute, Barakaldo, Spain

[2]Departamento de Microbiología y Parasitología, Facultad de Farmacia, UCM & Instituto Ramón y Cajal de Investigaciones Sanitarias (IRYCIS), Madrid, Spain

[3]Ikerbasque, The Basque Foundation for Science, Bilbao, Spain

[4]Institute for Cancer Research, Oslo University Hospital, Oslo, Norway

[5]Department of Pathology, Cruces University Hospital, Barakaldo, Spain

Correspondence
Rafael Pulido, Biocruces Bizkaia Health Research Institute, Barakaldo, Spain.
Email: rpulidomurillo@gmail.com and rafael.pulidomurillo@osakidetza.eus

Funding information
The Norwegian Research Council, Grant/Award Number: 239813; Ministerio de Economía y Competitividad (Spain and Fondo Europeo de Desarrollo Regional), Grant/Award Numbers: SAF2016-79847-R, and BIO2016-75030; Comunidad de Madrid and European Structural and Investment Funds, Grant/Award Number: S2017/BMD-3691 (InGEMICS-CM)

Abstract

The *PTEN* tumor suppressor gene is mutated with high incidence in tumors and in the germline of patients with cancer predisposition or with macrocephaly associated with autism. *PTEN* nonsense mutations generating premature termination codons (PTC) and producing nonfunctional truncated PTEN proteins are frequent in association with human disease. However, there are no studies addressing the restoration of full-length PTEN proteins from the PTC-mutated *PTEN* gene by translational readthrough. Here, we have performed a global translational and functional readthrough analysis of the complete collection of *PTEN* PTC somatic or hereditary mutations found in tumors or in the germline of patients (disease-associated PTEN PTCome), and we set standards for the analysis of the potential of readthrough functional reconstitution in disease-relevant genes. Our analysis indicates that prevalent pathogenic *PTEN* PTC mutations are susceptible to PTEN functional restoration in response to readthrough-inducing compounds. Comprehensive readthrough analyses of disease-associated PTComes will be valuable tools for the implementation of readthrough-based precision interventions in specific groups of patients.

KEYWORDS

nonsense mutation, premature termination codon, translational readthrough, tumor suppressor

1 | INTRODUCTION

The tumor suppressor gene *PTEN* (MIM# 601728) is frequently mutated in human tumors, as well as in the germline of patients with hereditary tumor syndromes (mainly, Cowden Syndrome and Bannayan-Riley-Ruvalcaba Syndrome, MIM# 158350; grouped as PHTS, PTEN Hamartoma tumor syndrome) and with macrocephaly/autism syndrome (PTEN-ASD, PTEN autism spectrum disorder, MIM# 605309) (Alvarez-Garcia et al., 2019; Pulido et al., 2019; Yehia et al., 2020). PTEN exerts its major tumor-suppressive functions by dephosphorylation of the 3' position from phosphatidylinositol (3,4,5)-trisphosphate (PIP3), counteracting the activity of the

Sandra Luna, Leire Torices, Janire Mingo, and Laura Amo contributed equally to this study.

prosurvival PI3K/AKT pathway and downregulating cell growth, invasion, and migration (Lee et al., 2018; Milella et al., 2015; Ngeow & Eng, 2020; Pulido, 2015; Worby & Dixon, 2014). Many *PTEN* mutations associated with cancer confer loss of PTEN phosphatase activity or destabilization of PTEN protein (Andrés-Pons et al., 2007; Georgescu et al., 2000; Han et al., 2000; Rodríguez-Escudero et al., 2011; Spinelli et al., 2015). A large number of these *PTEN* pathogenic mutations are missense mutations causing single amino acid substitutions at the N-terminal phosphatase PTEN domain and, to a lesser extent, at the C-terminal C2 PTEN domain. In addition, *PTEN* nonsense mutations creating a premature termination codon (PTC) at the PTP and C2 PTEN domains are also frequent in tumors and in patients, and generate unstable and nonfunctional truncated PTEN proteins (Andrés-Pons et al., 2007; Georgescu et al., 1999; Vazquez et al., 2000). Hence, intervention strategies based on the reconstitution of full-length PTEN expression could be beneficial for patients with *PTEN* nonsense mutations.

Translational readthrough of PTCs occurs during protein biosynthesis and consists of the incorporation of an amino acid in a position corresponding to an abnormal stop codon, allowing the translation to continue until the next stop codon in the coding region of a gene. Thus, readthrough induction constitutes a potential intervention to reconstitute in PTC-targeted patients the expression of full-length functional proteins (Asiful Islam et al., 2017; Keeling et al., 2014; Morais et al., 2020). Different small molecules, mainly aminoglycoside antibiotics but also nonaminoglycoside compounds, have the capability to induce readthrough to a variable extent, with low effects on the fidelity of recognition of the natural stop codons (Friesen et al., 2017; Nagel-Wolfrum et al., 2016; Peltz et al., 2013). However, the heterogeneity in the efficacy, bioavailability, and toxicity of the readthrough-inducing compounds, as well as the requisite of protein functional reconstitution upon readthrough induction, prompts the necessity of dedicated experimental validation and optimization of readthrough in specific protein targets before this approach enters the clinic as an efficient therapy (Dabrowski et al., 2018). In this regard, the identification of readthrough-inducing compounds of high efficacy and low toxicity in the clinic is currently under intense scrutiny (Baradaran-Heravi et al., 2016; Bidou et al., 2017; Campofelice et al., 2019; Liang et al., 2017; Sabbavarapu et al., 2016). The potential efficacy of readthrough therapies is directly affected by the readthrough response of the specific PTC carried on the mutated gene, which is mainly influenced by the nucleotide context surrounding the PTC. Thus, precise information on the readthrough response of each PTC on a given gene is important to predict effectiveness. In addition, it is also important to know how the function of the targeted protein is affected upon readthrough by the incorporation of variable amino acids at the PTC position, a property intrinsic to the readthrough phenomena (Dabrowski et al., 2015; Floquet et al., 2012; Roy et al., 2016; Xue et al., 2017). Together, this makes necessary precise studies that provide information from groups of patients harboring specific nonsense mutations at specific genes.

PTC in tumor suppressor genes are frequently associated with human cancer, and the potential of therapeutic readthrough has been evaluated for several PTC affecting *TP53* and *APC* tumor suppressor genes, with promising results of functional restoration of TP53 and APC functions (Baradaran-Heravi et al., 2016; Floquet, Deforges, et al., 2011; Floquet, Rousette, 2011; Keeling & Bedwell, 2002; Zilberberg et al., 2010). However, no global readthrough studies have been reported for these or other cancer-relevant human genes. The *PTEN* gene is among the tumor suppressor genes most frequently mutated in human cancer and is highly targeted by PTC (H. Tan et al., 2015), but the potential of PTEN readthrough-based interventions has not been disclosed. Here, we present a global analysis of the readthrough response and functional reconstitution of the complete repertoire of PTC targeting the *PTEN* gene in tumors and in PHTS/PTEN-ASD patients. Our results unveil that prevalent pathogenic *PTEN* PTC mutations are susceptible to PTEN functional restoration upon readthrough induction. Furthermore, we set the basis of global readthrough studies on genes targeted by PTC in human disease, and we propose a readthrough efficiency score, which could help to define the potential of readthrough interventions in specific groups of patients.

2 | MATERIALS AND METHODS

2.1 | In silico PTCome analysis and statistics

To help in the in silico and experimental analysis of gene PTComes, we provide a simple Phyton program (PTCMAKER) that lists the stop codons generated by single-nucleotide substitutions from a given nucleotide sequence (potential PTCome), as well as standardized mutagenic primers to generate those mutations by polymerase chain reaction (PCR) oligonucleotide site-directed mutagenesis. The program can be run online, or on Windows and GNU/Linux as standalone GUI executable files. All details, source code, and information can be found at https://github.com/compneurobilbao/stop-codon-pulido-17. The list of stop codons generated by single-nucleotide substitutions found in *PTEN* gene in association with human disease (disease-associated PTEN PTCome) was obtained by database (HGMD Professional, 2020 [https://digitalinsights.qiagen.com/products-overview/clinical-insights-portfolio/human-gene-mutation-database/]; Stenson et al., 2017; and COSMIC, Catalogue of Somatic Mutations in Cancer, Wellcome Trust Sanger Institute, v90 [https://cancer.sanger.ac.uk/cosmic; Tate et al., 2019]) and literature search, and contains, to the best of our knowledge, all the different *PTEN* PTC found in tumor samples or in the germline of patients. The distribution of PTC along PTEN protein was visualized by Kernel density plots. The relative frequencies of somatic *PTEN* PTC mutations come from the COSMIC database. The relative frequencies and quantitation of germline *PTEN* PTC mutations come from literature retrieval, as listed in the Supplementary list of references, and from HGMD Professional and references therein. For nonsense/missense germline mutation ratio comparison, data are from references (Bubien et al., 2013; Pilarski et al., 2011; M. H. Tan et al., 2011). Statistical analysis of PTComes and readthrough efficiency data was performed by Fisher´s exact test, two-tailed, using GraphPad.

2.2 | Cell lines, cell culture, transfections, and reagents

Simian kidney COS-7 cells (PTEN wild-type) were grown in Dulbecco's modified Eagle's medium (DMEM) containing high glucose supplemented with 5% heat-inactivated fetal bovine serum (FBS), 1 mM L-glutamine, 100 U/ml penicillin, and 0.1 mg/ml streptomycin. Human glioblastoma U87MG cells (PTEN null) were grown in DMEM containing high glucose supplemented with 10% heat-inactivated FBS, 1 mM L-glutamine, 1 mM sodium pyruvate, 1% nonessential amino acids, 100 U/ml penicillin, and 0.1 mg/ml streptomycin. Cells were grown at 37°C and 5% CO_2. COS-7 cells were transfected by the DEAE-dextran method or using GenJet (SignaGen Laboratories), and U87MG cells were transfected using Lipofectamine (Thermo Fisher Scientific). Transfected cells were cultured for 24 h, followed by incubation in the absence or in the presence of readthrough inducers, as indicated. Readthrough-inducing reagents were as follows: G418 (Geneticin, #345810; Merck Sigma Aldrich), gentamicin (#345815; Merck Sigma Aldrich), amikacin (#A0368000; Merck Sigma Aldrich), tobramycin (#T1783; Merck Sigma Aldrich), and erythromycin (#E5389 Merck Sigma Aldrich).

2.3 | Plasmids and mutagenesis

pRK5 PTEN, pRK5 PTEN-GFP, pYES2 PTEN, YCpLG myc-p110α-CAAX, and pSG5 HA-AKT1 plasmids have been previously described (Andrés-Pons et al., 2007; Gil et al., 2006; Mingo et al., 2018). pRK5 PTEN M35 (lacking residues 1–34; PTEN 35-403) was made by one-step deletion PCR oligonucleotide site-directed mutagenesis, as described (Luna et al., 2016). Nucleotide substitution mutagenesis was made by PCR oligonucleotide site-directed mutagenesis as described (Mingo et al., 2016). All mutations were confirmed by DNA sequencing. Amino acid numbering for PTEN variants corresponds to reference sequence from accession number NP_000305.

2.4 | Immunoblotting, determination of readthrough efficiency, and fluorescence microscopy

Immunoblotting was performed as described (Mingo et al., 2018). Briefly, whole-cell protein extracts from COS-7 or U87MG cells overexpressing ectopic PTEN variants were prepared by cell lysis in ice-cold M-PER™ lysis buffer (Thermo Fisher Scientific) supplemented with PhosSTOP phosphatase inhibitor and complete protease inhibitor cocktails (Roche), followed by centrifugation at 15,200*g* for 10 min and collection of the supernatant. Cell lysates were subjected to sodium dodecyl sulfate-polyacrylamide gel electrophoresis (10% or 12%). Proteins (50–100 μg) were resolved under reducing conditions and transferred to polyvinylidene difluoride membranes (Immobilon-FL). Immunoblotting was performed using the anti-PTEN C-terminal 6H2.1 monoclonal antibody (PTEN residues 392–398) (Mingo et al., 2019), a polyclonal anti-PTEN N-terminal antibody (PTEN residues 1–15) (Gil et al., 2006), anti-phospho-Ser473-AKT and anti-AKT (both from Cell Signaling Technologies), and anti-glyceraldehyde 3-phosphate dehydrogenase (Santa Cruz Biotechnology). Secondary antibodies conjugated with fluorochrome were anti-rabbit or anti-mouse IgG-IRDyeR 800CW (or IgG-Alexa FluoR 680) (LI-COR Biosciences). For determination of readthrough efficiency and readthrough efficiency scores, the full-length PTEN protein bands were quantified using an Image Studio™ software with Odyssey® CLx Imaging System (LI-COR Biosciences). Readthrough efficiency was determined as the percentage of each full-length PTEN PTC variant translated under readthrough-inducing conditions compared to the translation of PTEN wild-type (100%). For determination of phospho-AKT (Ser473) content from COS-7 cells upon PTEN readthrough induction, bands were quantified as indicated above, and results are shown as the ratio pAKT/AKT. For all comparative results shown, blots were derived from the same experiment and were processed in parallel. For PTEN-GFP readthrough induction, 24 h posttransfection, COS-7 cells were incubated in the presence of G418 (200 μg/ml) for an additional 24 h, and then were directly visualized by standard fluorescence microscopy, as described (Mingo et al., 2018). For the determination of readthrough efficiencies and phospho-AKT content, at least two independent experiments were performed for each mutation, and results are shown as the mean ± *SD*.

2.5 | Yeast functional assays and determination of functional scores and readthrough efficiency scores

Heterologous expression and functional analysis of PTEN variants in the *Saccharomyces cerevisiae* yeast strain YPH499 (*MAT*a *ade2-101 trp1-63 leu2-1 ura3-52 his3-Δ200 lys2-801*) was performed as described (Cid et al., 2008; Gil et al., 2016; Rodriguez-Escudero et al., 2015). In these assays, yeast growth is dependent on the presence of catalytically active human PTEN, which counteracts the toxic effect of a hyperactive mammalian myc-p110α-CAAX enzyme (*PIK3CA* gene) (Rodríguez-Escudero et al., 2005). YPH499 yeast cells were grown in synthetic complete (SC) medium [containing 0.17% yeast nitrogen base without amino acids, 0.5% ammonium sulfate supplemented with appropriate amino acids and nucleic acid bases, and 2% glucose (SD), raffinose (SR) (noninducing conditions of heterologous protein expression), or galactose (SG) (inducing conditions of heterologous protein expression) as required] and transformed by standard procedures. For drop growth assays, three serial 1/10 dilutions of transformant cells were spotted onto SD or SG plates lacking the corresponding auxotrophic markers, and growth was monitored after 2–3 days at 30°C (Rodríguez-Escudero et al., 2011). For GFP-AKT1 membrane localization, as a surrogate indicator of cellular PIP3 (which is converted to PIP2 by catalytically active PTEN), transformant cells were grown in liquid SR media lacking the corresponding auxotrophic markers, and 2% galactose was added for 6–8 h to induce the expression of the heterologous proteins, followed by GFP-AKT1 visualization by standard fluorescence microscopy (Rodríguez-Escudero et al., 2011). Functional score of each

PTEN variant was determined by drop growth assays and reflects the functional competence of each variant to counteract the toxic action of p110α-CAAX in the yeast, in comparison with PTEN wt (1, functional activity similar to PTEN wild-type; 0.5, functional activity reduced; 0, very low or absent functional activity). In addition, functional scores were generated from the high-resolution map of the functional effects on PTEN mutations reported by Mighell et al. (2018) (built using our yeast heterologous expression system). We define the readthrough efficiency score taking into consideration the following variables: The readthrough efficiency for each PTC, the amino acid incorporation frequency (AIF_1, AIF_2, and AIF_3) of the most frequently incorporated amino acids for each PTC (TGA, substitutions to Arg [R; 0.645 frequency], Trp [W, 0.179], and Cys [C, 0.177]; TAG, substitutions to Gln [Q, 0.865], Tyr [Y, 0.108], and Lys [K, 0.02]; TAA, substitutions to Gln [Q, 0.52] and Tyr [Y, 0.479], as reported by Roy et al., 2016), and the functional scores of the most frequently generated PTEN variants in each case (FS_1, FS_2, and FS_3). The readthrough efficiency score of the disease-associated PTEN PTCome is calculated as follows:

$$\text{Readthrough efficiency score} = \text{Readthrough efficiency} \times [([FS_1 \times AIF_1] + [FS_2 \times AIF_2] + [FS_3 \times AIF_3]).$$

All score numbers are included in Tables S1 and 2.

3 | RESULTS AND DISCUSSION

3.1 | Disease-associated PTEN PTCome

Nonsense single-nucleotide substitutions targeting the *PTEN* gene in human tumors, which generate PTC in the *PTEN* gene-coding region, constitute about 30% of the total of single-nucleotide mutations found in this gene in association with neoplasias [estimations are from the nucleotide sequence (NM_000314) encoding the canonical PTEN isoform (NP_000305; 403 amino acids); COSMIC database]. In addition, the *PTEN* gene is also frequently targeted by PTC mutations in the germline of PHTS and PTEN-ASD patients, with estimations of about 50% of single-nucleotide substitution reported cases (Bubien et al., 2013; Pilarski et al., 2011; M. H. Tan et al., 2011). We name all possible PTC generated by single-nucleotide substitutions in *PTEN* complementary DNA (cDNA) as the *potential PTEN PTCome*, and the fraction of the different *PTEN* PTC mutations found in association with human disease as the *disease-associated PTEN PTCome* (Figure 1a). We provide an easy-to-use program that helps in the in silico and experimental comparative analysis of potential and disease-associated PTComes (PTCMAKER; https://github.com/compneurobilbao/stop-codon-pulido-17). The potential PTEN PTCome includes 183 different PTC (TAA, 42.6%; TAG, 33.3%; TGA, 24%), distributed all along the PTEN protein [PTP domain (residues 1–185), 51.5% PTC, 0.5 PTC/residue; C2 domain (residues 186–353), 39.5% PTC, 0.43 PTC/residue; C-terminal tail (residues 354–403), 9% PTC, 0.34 PTC/residue]. These potential PTC arise from single-nucleotide substitutions from 146 different codons, including 17 out of the 18 potential PTC-generating codons (the TCG codon is not present in *PTEN* gene). Up-to-date, the reported disease-associated PTEN PTCome includes 141 different PTC (TAA, 43.2%; TAG, 31.2%; TGA, 25.5%) (Figure 1a and Table S1). These relative qualitative PTC frequencies are slightly different from the global frequencies of the distinct PTC found in human genes in association with genetic diseases (TAA, 21.1%; TAG, 40.4%; TGA, 38.5%) (Atkinson & Martin, 1994; Mort et al., 2008). Disease-associated PTEN PTC distributes almost equally in both the PTP (56.7% PTC, 0.43 PTC/residue) and the C2 (43.3% PTC, 0.36 PTC/residue) PTEN domains, whereas PTC mutations are not found in association with disease in the positions corresponding to the last 50 residues from the PTEN C-terminal tail (Figure 1a and Table S1 and S2). These observations suggest that elimination of PTEN C-terminal tail by premature protein truncation is not directly linked with human disease and reinforces the notion of a regulatory rather than an essential role for this PTEN C-terminal region in the control of cell homeostasis (Gil et al., 2007; Leslie & Foti, 2011; Song et al., 2012; Sotelo et al., 2015). No apparent bias is observed for the domain distribution of the somatic or the germline PTC, as visualized by Kernel density plots (Figure S1).

From a quantitative perspective, the relative number of germline *PTEN* PTC mutations found in patients is enriched when compared with the number of somatic *PTEN* PTC mutations found in tumor samples both in the PTP and the C2 domains. In addition, the relative number of TGA PTC found in the germline of patients (70% of total germline PTC mutations) is also higher than the relative number of somatic TGA PTC found in tumors (49% of total somatic PTC mutations) (Figure S1 and Table S2). There are specific *PTEN* nonsense mutations very frequently found in tumors and in PHTS patients, mainly as the consequence of the high mutability CpG to TpG transition targeting specific *PTEN* codons. For instance, the CGA to TGA mutations creating the PTC R130X, R233X, and R335X [c.388C>T, p.(Arg130Ter); c.697C>T, p.(Arg233Ter); c.1003C>T, p.(Arg335Ter)] constitute, together, about 37% of total *PTEN* PTC mutations found in human tumors, and about 52% of the estimation of *PTEN* PTC mutations found in PHTS patients. Noticeably, a much higher relative frequency of germline R335X PTC mutation is observed when compared to tumor-associated R335X PTC mutation (Figure 1b). In summary, three particular *PTEN* mutations generating PTC (R130X, R233X, and R335X) account for about 10%–25% of *PTEN* single-nucleotide substitutions found in patients. In sporadic tumors, this trend of mutation frequency is particularly relevant in the case of cancers with a high incidence of *PTEN* mutations, such as endometrial cancer (37% incidence) or glioblastoma (13%) (COSMIC database). Together, these observations highlight the clinical importance of *PTEN* PTC mutations in specific groups of cancer patients.

3.2 | Induction of translational readthrough of PTEN

Inducible translational readthrough of PTC is a suitable approach to reconstitute the expression of full-length proteins encoded by

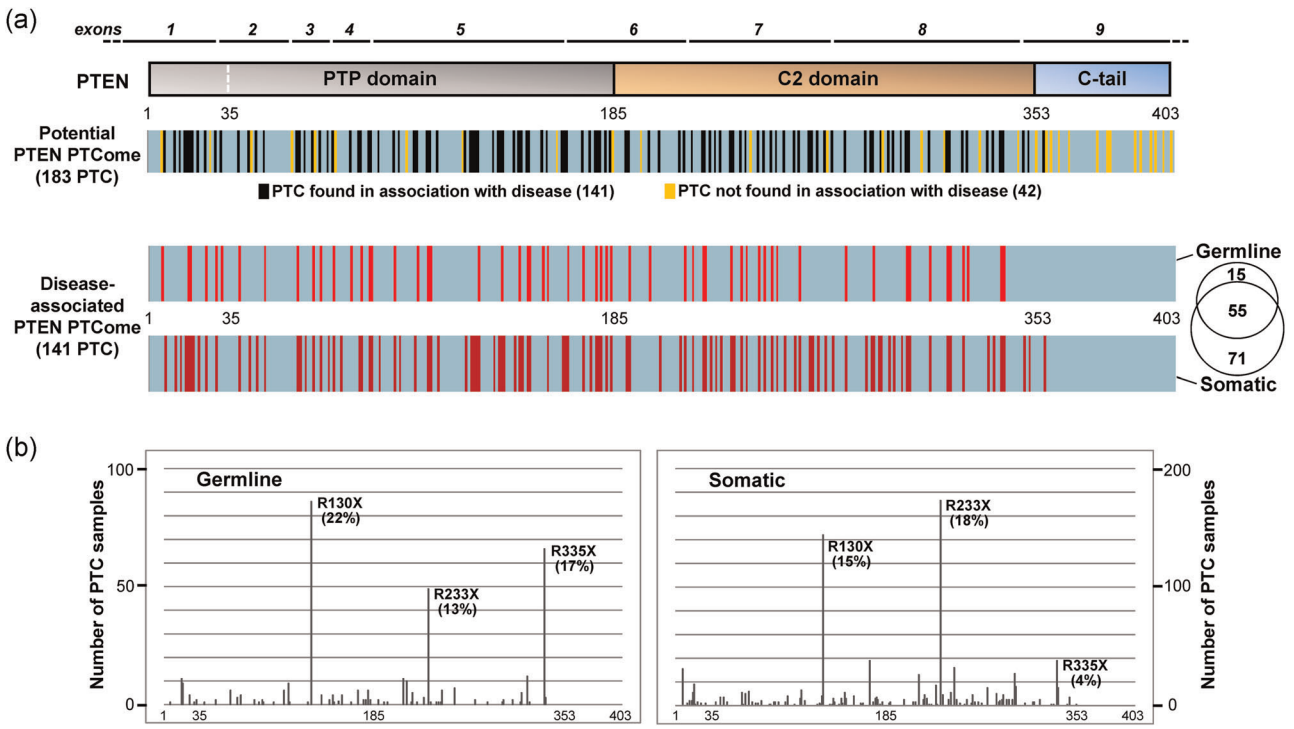

FIGURE 1 PTEN PTCome. (a) Depiction of *PTEN* gene exons, PTEN protein domain composition, and distribution of *PTEN* PTC (premature termination codons). At the top, a depiction is shown of the PTEN protein domain composition (numbers correspond to PTEN amino acid numbering: PTP domain, amino acids 1–185 [amino acid 35 corresponds to Met35]; C2 domain, amino acids 186–353; C-terminal tail, amino acids 354–403), and the regions encoded by the different *PTEN* gene exons (italic numbers) are indicated. The distribution on PTEN of the 183 PTC, which can be generated by single-nucleotide substitutions from *PTEN* nucleotide sequence (potential PTEN PTCome) is shown in the solid bar below the PTEN protein depiction. In black, PTC that have been found up-to-date associated with the disease (141 PTC). In yellow, PTC that have not been found up-to-date associated with the disease (42 PTC). At the bottom, depictions are shown of the distribution in PTEN protein of the germline and somatic PTC (marked in red) found in the *PTEN* gene in association with the disease (disease-associated PTEN PTCome). Out of 141 different PTC, 15 PTC have only been found in the germline of patients, 71 PTC have only been found in tumor samples, and 55 PTC have been found from both sources. (b) Frequency of germline and somatic PTC found in *PTEN* gene in association with disease. In the left panel, the number of times each PTC has been found in the germline of patients is represented (data are from HGMD Professional database, 2020[for those PTC only found one time] and literature retrieval [see references under Supporting Information Material]). In the right panel, the number of times each PTC has been found in tumor samples (somatic mutations) is represented (data are from the COSMIC database [v90])

PTC-targeted genes. Aminoglycoside antibiotics, including G418 (Geneticin) and gentamicin, have been reported as readthrough inducers of different PTC-targeted genes in a variety of cell types (Hermann, 2007; Midgley, 2019). We tested the efficacy of G418 to induce readthrough in PTEN using COS-7 and U87MG cell lines transiently transfected with cDNA plasmids encoding the R130X (TGA) and R233X (TGA) *PTEN* mutations frequently found in association with human disease. As shown, G418 efficiently induced readthrough from the two mutations in both cell lines, as monitored by immunoblot with an anti-PTEN C-terminal mAb (Figure 2a). To assess the specificity of the G418-induced readthrough, we cotransfected the PTEN-containing pRK5 plasmid (pRK5; lacking a Neomycin [Neo]-resistance gene, whose protein product [aminoglycoside-3′-phosphotransferase IIa] inactivates G418; Wright & Thompson, 1999) with additional pRC/CMV or pSG5 empty plasmids (pRc/CMV; carrying Neo-resistance gene; pSG5; lacking Neo-resistance gene). Cotransfection with pRc/CMV resulted in blockade of G418-induced PTEN readthrough, indicating specificity in the effect of G418 on PTEN reconstituted expression (Figure 2b). Next, we assessed the readthrough induced by G418 and gentamicin on some other representative human PTEN variants containing PTC, using two different anti-C-terminal or anti-N-terminal PTEN antibodies. Both G418 and gentamicin triggered PTEN readthrough, generating full-length PTEN proteins at a variable extent depending on the specific PTC. The induced readthrough was higher with G418, although it could also be noticeable with gentamicin. Some PTEN PTC variants (such as R335X) rendered low levels of PTEN C-terminal-truncated proteins in the absence of the readthrough inducers, as detected by their reactivity with the anti-N-terminal-PTEN antibody, but not with the anti-C-terminal PTEN antibody (Figure 2c). Note that the stability of PTEN C-terminal truncations is compromised, which impedes their detection. Thus, a detailed analysis of the expression of the different *PTEN* PTC mutations showed a gradual decrease in the expression levels of the resulting PTEN C-terminal-truncated proteins, with PTC beyond the 219 residues being undetectable (Figure 2d). This is in agreement with the

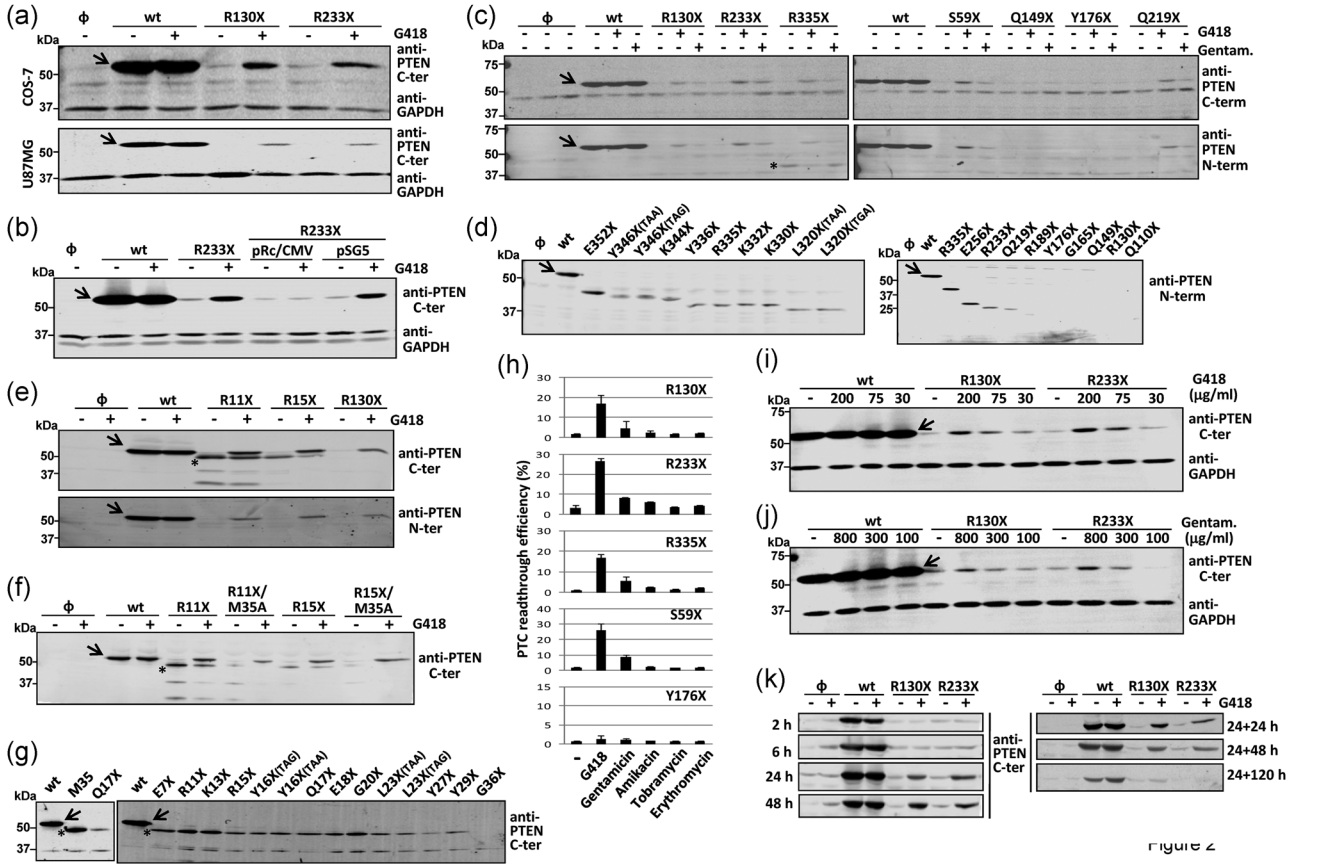

FIGURE 2 Translational readthrough of *PTEN* PTC (premature termination codons) mutations. (a) Readthrough-induced expression of the frequently disease-associated *PTEN* R130X [p.(Arg130Ter)] and R233X [p.(Arg233Ter)] mutations. COS-7 or U87MG cells were transfected with pRK5 plasmids containing the different *PTEN* variants, and 24-h posttransfection cells were kept untreated or incubated in the presence of G418 (200 μg/ml) for an additional 24 h, as indicated. Ø, empty vector. PTEN proteins were resolved in 10% sodium dodecyl sulfate-polyacrylamide gel electrophoresis (SDS-PAGE) gels and were detected by immunoblot using the anti-C-terminal PTEN 6H2.1 mAb. Detection of glyceraldehyde 3-phosphate dehydrogenase (GAPDH) with anti-GAPDH antibody is shown as a control. The arrow (→) in the distinct panels indicates the migration of full-length PTEN. (b) Specificity of G418-induced PTEN readthrough. COS-7 cells were transfected with pRK5 plasmids as in (a) or were cotransfected with pRK5 plasmids and the empty vectors pRc/CMV or pSG5, as indicated. Cells were kept untreated or treated with G418, and PTEN and GAPDH proteins were detected as in (a). Ø, empty vector. (c) Readthrough-induced expression of PTEN PTC mutations. COS-7 cells were transfected with several *PTEN* PTC mutations, as in (a), and 24-h posttransfection cells were kept untreated or incubated in the presence of G418 (200 μg/ml) or gentamicin (Gentam., 800 μg/ml) for an additional 24 h, as indicated. PTEN proteins were resolved in 10% SDS-PAGE gels and were detected by immunoblot using separately the anti-C-terminal PTEN 6H2.1 mAb or anti-N-terminal PTEN antibody, as indicated. The asterisk (*) indicates the migration of the R335X [p.(Arg335Ter)] PTEN-C-terminal-truncated protein. Ø, empty vector. (d) Expression of PTEN C-terminal-truncated proteins from the corresponding *PTEN* PTC variants. COS-7 cells were transfected with *PTEN* PTC mutations targeting PTEN C-terminal region, as in (a), and PTEN proteins were resolved in 10% SDS-PAGE (left panel) or 12% SDS-PAGE (right panel) gels and were detected by immunoblot using an anti-N-terminal PTEN antibody. Ø, empty vector. (e,f) Readthrough-induced expression of *PTEN* PTC mutations targeting PTEN N-terminal region. COS-7 cells were transfected as in (a). Cells were kept untreated or treated with G418, and PTEN proteins were detected by immunoblot using separately the anti-C-terminal PTEN 6H2.1 mAb or an anti-N-terminal PTEN antibody, as indicated. The asterisk (*) indicates the migration of the PTEN-N-terminal-truncated protein. Ø, empty vector. (g) Expression of PTEN N-terminal-truncated proteins from the corresponding *PTEN* PTC variants. COS-7 cells were transfected with *PTEN* PTC mutations targeting the PTEN N-terminal region, as in (a), and PTEN expression was detected by immunoblot using the anti-C-terminal 6H2.1 PTEN mAb. The asterisk (*) indicates the migration of the PTEN-N-terminal-truncated protein, as well as the migration of a PTEN protein lacking residues 1–34, whose translation starts in Met35 (PTEN 35-403; M35). (h) Quantification of readthrough-induced expression of *PTEN* PTC mutations. COS-7 cells were transfected and processed for PTEN expression as in (a). Cells were incubated in the presence of readthrough inducers for 24 h (G418, 200 μg/ml; gentamicin, 800 μg/ml; amikacin, 2 mg/ml; tobramycin, 800 μg/ml; erythromycin, 175 μg/ml). Data are shown as relative PTEN full-length expression, in comparison with PTEN wild-type (wt) (100%) (mean ± *SD* from two independent experiments), as determined by PTEN protein band quantification. (i,j) Dose–response of PTEN readthrough induction. COS-7 cells were transfected as in (a). Cells were kept untreated or treated with different doses of G418 or gentamicin (Gentam.), as indicated, and PTEN and GAPDH proteins were detected as in (a). (k) Time-course of PTEN readthrough response. COS-7 cells were transfected as in (a). Cells were kept untreated or treated with G418 (200 μg/ml) during the indicated time. In the left set of panels, cells were always in the presence of G418. In the right set of panels, cells were incubated 24 h in the presence of G418, followed by additional incubation in the absence of G418, as indicated. PTEN proteins were detected as in (a). In all cases, blots show one representative experiment from at least two independent experiments

reported lack of stability and function in cells of C-terminal-truncated PTEN proteins (Andrés-Pons et al., 2007; Georgescu et al., 1999). Upon readthrough-inducing conditions, the amount of C-terminal PTEN (R335X) truncated forms diminished concomitantly to the amount of PTEN full-length generated by the readthrough (Figure 2c).

PTEN variants with PTC located N-terminal with respect to Met35, such as R11X [c.31A>T, p.(Arg11Ter)], and R15X [c.43A>T, p.(Arg15Ter)], rendered a PTEN N-terminal-truncated protein, as revealed by its lack of reactivity with the anti-N-terminal-PTEN antibody (Figure 2e). The amount of the N-terminal PTEN truncated forms diminished upon readthrough induction. Substitution of Met35 by Ala (M35A experimental variant) [c.(103A>G; 104T>C), p.(Met35Ala)] resulted in the suppression of the synthesis of the N-terminal-truncated PTEN protein from the corresponding *PTEN* PTC mutations (R11X/M35A, R15X/M35A) (Figure 2e,f). Furthermore, the PTEN N-terminal-truncated protein comigrated with a PTEN protein starting at Met35 (Figure 2g). All *PTEN* PTC mutations before Met35 residue, but not the G36X mutation [c.106G>T, p.(Gly36Ter)], produced the N-terminal-truncated PTEN protein (Figure 2g). This demonstrates that PTEN Met35 residue is used to reinitiate translation when a PTC is present upstream of this amino acid. A similar PTC-dependent reinitiation of translation has been recently reported for the tumor suppressor p53, indicating that this could be a common phenomenon for proteins showing disease-associated PTC (Cohen et al., 2019). The presence of N- and C-terminal-truncated PTEN proteins arising from specific *PTEN* PTC mutations, add complexity to the molecular phenotypes associated with such mutations, which may be relevant for precision diagnosis of specific carrier patients. Importantly, induced readthrough decreased the amount of the disease-associated PTEN truncations and restored the expression of PTEN full-length protein.

Next, we tested additional readthrough inducers on several *PTEN* PTC variants, including aminoglycoside (G418, gentamicin, amikacin, and tobramycin) and nonaminoglycoside (erythromycin) compounds. The more potent readthrough inducer was G418, followed by gentamicin (Figure 2h). Dose and time-responses of readthrough induction by G418 and gentamicin on the *PTEN* variants R130X and R233X are shown in Figure 2i-k. The readthrough-inducing effect of G418 was sustained in the cells up to 48 h after the removal of G418 from the media (Figure 2k). In conclusion, readthrough of human *PTEN* variants frequently found in tumors and in patients can be efficiently achieved in cultured cells upon incubation with aminoglycoside readthrough inducers.

3.3 | Global readthrough analysis of the disease-associated PTEN PTCome

Readthrough is influenced by the specific identity of each PTC, as well as by the proximal nucleotide context sequence close to it in the messenger RNA (mRNA) (Linde & Kerem, 2008). To make a global estimation of the potential of readthrough to reconstitute PTEN full-length expression and function, we performed a comprehensive analysis of readthrough induction by G418 on the disease-associated PTEN PTCome (141 *PTEN* variants) (Figure 3a and Table S1). Full-length expression of the different *PTEN* PTC variants upon G418 readthrough induction ranged between 0% and 35% with respect to expression of PTEN wild-type, and we did not observe a clear bias in this *readthrough efficiency* (percentage of expression with respect to PTEN wild-type) when considering the position of the PTC along the *PTEN* mRNA sequence. A classification of PTC according to their readthrough response is shown in Table 1. Overall, about 4% of PTC displayed optimal readthrough efficiency (>20% expression with respect to PTEN wild-type), 17% displayed suboptimal readthrough efficiency (10%–20% expression), 21% displayed low readthrough efficiency (5%–9% expression), and 58% displayed very low

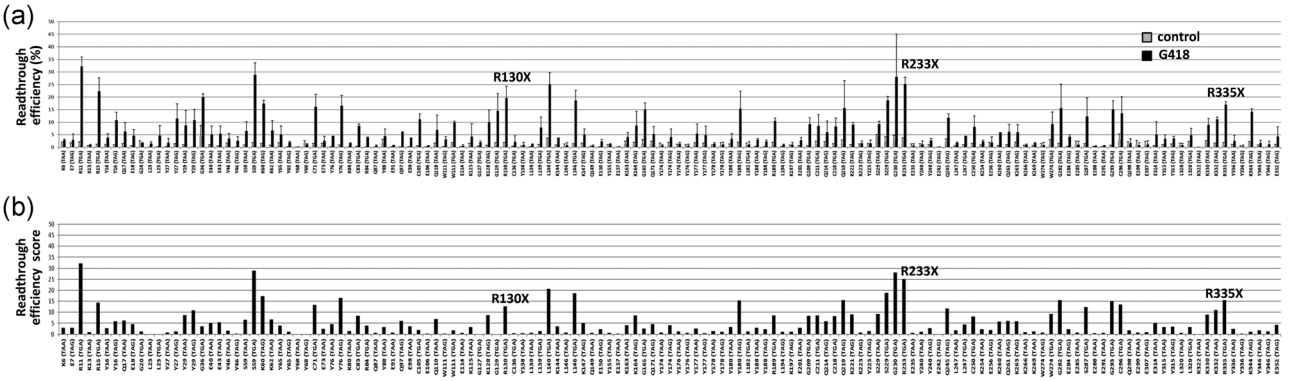

FIGURE 3 Global readthrough analysis of disease-associated PTEN PTCome. (a) Readthrough efficiency of disease-associated PTEN PTCome. Readthrough efficiency in response to G418 is shown, as the percentage of PTEN full-length expression with respect to PTEN wild-type expression, as in Figure 2h. Data are shown as mean ± *SD* from at least two independent experiments. (b) Readthrough efficiency score of disease-associated PTEN PTCome. Readthrough efficiency score was calculated as indicated under Section 2. The readthrough efficiency score adjusts the readthrough efficiencies according to the functional score of the predicted variants generated by readthrough. Functional scores are provided in Table S1. In both (a) and (b), the PTC (premature termination codon)-targeted residues are indicated, and the PTC are in brackets. The high-frequency R130X [p.(Arg130Ter)], R233X [p.(Arg233Ter)], and R335X [p.(Arg335Ter)] PTC are denoted

TABLE 1 Readthrough efficiency of disease-associated PTC (premature termination codon) types

PTC	*n*[a]	Readthrough efficiency[b]			
		Optimal	Suboptimal	Low	Very low
		6 (4.3%)	24 (17%)	30 (21.3%)	81 (57.4%)
TGA	36 (25.5%)	6 (100%)	14 (58.3%)	8 (26.7%)	8 (10%)
TAG	44 (31.2%)	0 (0%)	9 (37.5%)	9 (30%)	26 (32%)
TAA	61 (43.2%)	0 (0%)	1 (4.2%)	13 (43.3%)	47 (58%)

[a]Number and percentage of each PTC type in PTEN disease-associated PTCome.

[b]Readthrough efficiency is defined as the percentage of expression with respect to PTEN wild-type (100%): Optimal (>20% expression), suboptimal (10%–20% expression), low (5%–9% expression), and very low (0%–4% expression). The number and percentage of each PTC type are indicated.

readthrough efficiency (0%–4% expression) (Table 1). Remarkably, the prevalent *PTEN* PTC mutations R130X, R233X, and R335X displayed optimal or suboptimal readthrough (Tables S1 and 2). This reinforces the potential of PTEN readthrough-based interventions for specific groups of patients. Our comprehensive readthrough analysis of 141 different PTC in the PTEN-encoding mRNA allowed us to perform some comparative analysis in terms of optimal mRNA sequences for PTEN readthrough. The mean of the readthrough efficiencies for each PTC type were: TGA, 13.2% readthrough efficiency (range 1%–32%); TAG, 5.4% efficiency (range 0%–17%); TAA, 3% efficiency (range 0%–11%). Most of the PTC displaying optimal or suboptimal readthrough efficiency were TGA PTC (67%), followed by TAG (30%) and TAA (3%). On the contrary, the majority of PTC displaying low or very low readthrough efficiency were TAA PTC (54%), followed by TAG (32%) and TGA (14%), with only one TAA PTC displaying suboptimal readthrough efficiency (Table 1). In summary, TGA PTC was statistically associated with optimal or suboptimal readthrough efficiency, whereas TAA PTC was associated with low or very low readthrough efficiency (Table S3). When comparing pairs of PTC with identical surrounding nucleotide context (nucleotide substitutions rendering two different PTC from the same wild-type codon), an overall higher readthrough was observed for TGA versus TAA (12% readthrough efficiency vs. 3.4%, all TGA displayed higher readthrough, out of seven PTC pairs), and for TGA versus TAG (9.5% efficiency vs. 1.9%, all TGA displayed higher readthrough, out of two pairs). In the case of TAG versus TAA (5.5% efficiency vs. 3.1%, seven TAG displayed higher readthrough, out of 17 PTC pairs), there were abundant PTC pairs with similar readthrough efficiency. Our global findings are in agreement with previous readthrough comparative studies using different mRNAs or artificial reporter proteins, which showed a readthrough efficiency that follows the PTC order TGA>TAG>TAA but it is also influenced by the proximal nucleotide sequence (Bidou et al., 2004; Howard et al., 2000; Manuvakhova et al., 2000). In this regard, a cytosine (C) nucleotide at position +4 (+1 being the first nucleotide in the PTC) has been proposed as optimal for a readthrough. In our global PTEN readthrough analysis, the +4 nucleotide was a C in nine out of the 30 PTC (30%) displaying optimal or suboptimal readthrough, and in 15 out of the 111 PTC (13.5%), displaying low or very low readthrough. We tested whether mutating the +4 nucleotide to C could improve the readthrough efficiency of a selection of *PTEN* TGA PTC (TGAC mutations; PTC is underlined), including some showing very low readthrough (Figure 4). As shown, the readthrough of four out of nine TGA was increased by incorporating a C at position +4, when comparing to the +4 wild-type wt sequence or to any of the two other nucleotides at this position (Figure 4a,b). This indicates that the +4 C nucleotide may favor readthrough, but only in the appropriate nucleotide sequence context. Importantly, the enhancement in readthrough associated with the presence of +4 C was observed with several aminoglycoside readthrough-inducers (Figure 4c), suggesting the existence of highly optimal readthrough nucleotide sequences shared by different readthrough-inducing compounds. This could be important for the prediction of the potential readthrough response of a specific disease-associated PTC. An adenine (A) nucleotide at position −1 has also been proposed to favor readthrough (Tork et al., 2004). In our study, the −1 nucleotide was an A in seven out of the 30 PTC (23%) displaying optimal or suboptimal readthrough, with six PTC showing A at −1 and C at +4 positions (see legend for Table S1). However, 35 out of 111 PTC (31.5%) showing low- or very low readthrough harbored an A at −1 position, with nine PTC displaying A at −1 and C at +4 positions (Table S1). Together, our results indicate that, in the context of full-length protein translation, TGAC PTEN nucleotide sequences display a more likely highly optimal or suboptimal response to readthrough inducers. Nevertheless, individual testing is required to determine the readthrough potential of each combination of PTC and readthrough-inducer compound.

3.4 | Activity of readthrough PTEN variants and readthrough efficiency score

Incorporation during translational readthrough of amino acids encoded by near-cognate codons with respect to the wild-type codon targeted by the PTC mutation may affect the function of the resulting full-length protein. This is crucial in the case of proteins like PTEN, which display impaired functions as the consequence of a large variety of single amino acid substitutions along its peptide sequence. To address this issue from a global perspective, we analyzed the in vivo function of PTEN variants potentially generated by readthrough using a previously validated yeast heterologous system,

TABLE 2 Readthrough analysis of PTEN PTC frequently associated with the disease

Amino acid[a]	DNA variant[b]	Amino acid substitution[b]	Germline frequency[c]	Somatic frequency[d]	PTC[e]	Readthrough efficiency[f]	Functional score[g]	Readthrough efficiency score[h]
Q17	c.49C>T	p.(Gln17Ter)/Q17X	2.3	2.2	TAT TAA GAG	6.2 ± 3.6	1/1	6.2
E106	c.316G>T	p.(Glu106Ter)/E106X	1.5	0.2	TGT TAA GAT	0.6 ± 0.1	1/0	0.3
Q110	c.328C>T	p.(Gln110Ter)/Q110X	2.3	0.6	GAC TAA TGG	6.9 ± 5.8	1/1	6.9
R130	c.388C>T	p.(Arg130Ter)/R130X	21.9	14.8	GGA TGA ACT	19.6 ± 4.8	1/0/0	12.6
E157	c.469G>T	p.(Glu157Ter)/E157X	1.3	0.7	GGG TAA GTA	0.3 ± 0.1	1/1	0.3
Q171	c.511C>T	p.(Gln171Ter)/Q171X	1.5	3.8	AGT TAG AGG	5.3 ± 3.0	1/0/0	4.6
C211	c.633C>A	p.(Cys211Ter)/C211X	2.8	0.3	ACT TGA AAT	8.5 ± 4.5	1/1/1	8.5
Q214	c.640C>T	p.(Gln214Ter)/Q214X	2.6	2.7	CCT TAG TTT	5.9 ± 4.6	1/1/1	5.9
Q219	c.655C>T	p.(Gln219Ter)/Q219X	1.3	0.9	TGC TAG CTA	15.6 ± 11.0	1/1/1	15.6
R233	c.697C>T	p.(Arg233Ter)/R233X	12.6	17.9	ACA TGA CGG	25.2 ± 2.7	1/1/1	25.2
Q245	c.733C>T	p.(Gln245Ter)/Q245X	1.5	3.6	CCT TAG CCG	11.7 ± 1.7	1/1/1	11.7
E256	c.766G>T	p.(Glu256Ter)/E256X	1.8	0.5	GTA TAG TTC	1.9 ± 2.3	1/1/1	1.9
L320	c.959T>G	p.(Leu320Ter)/L320X	2.1	0.4	ACT TGA ACA	4.8 ± 2.7	0.5/1/1	2.7
R335	c.1003C>T	p.(Arg335Ter)/R335X	17	4.3	AAC TGA TAC	17.0 ± 1.1	1/0.5/1	15.5

Abbreviations: HGMD, Human Genome Mutation Database; HGVS, Human Genome Variation Society; PTC, premature termination codons.

[a]Amino acids whose coding codons are frequently substituted by PTC in association with the disease are indicated using the amino acid one-letter code. Amino acid numbering is according to NP_000305.

[b]DNA variants and amino acid substitutions are indicated following HGVS recommended nomenclature, as well as with single-letter code amino acid nomenclature. Nucleotide numbering is according to NM_000314.

[c]Frequency (%) of PTC found in the germline of patients, based on literature retrieval, as listed in the Supplementary list of references, and on HGMD Professional.

[d]Frequency (%) of PTC found in tumor samples, based on the COSMIC database.

[e]PTC are underlined and flanked by the adjacent codons.

[f]Readthrough efficiency in response to G418 is provided, as the percentage of expression with respect to PTEN wild-type.

[g]Functional score for each potential readthrough-generated PTEN variant was obtained as indicated under Section 2. Functional scores are indicated in the following order of amino acid variants: TGA, R/W/C; TAG, Q/Y/K; TAA, Q/Y. 1, functional activity similar to PTEN wild-type; 0.5, functional activity reduced; 0, very low or absent functional activity. See Figure 4 for examples of functional scores.

[h]Readthrough efficiency score results from adjusting the readthrough efficiency according to the functional scores of the variants generated by readthrough. See complete definition under Section 2.

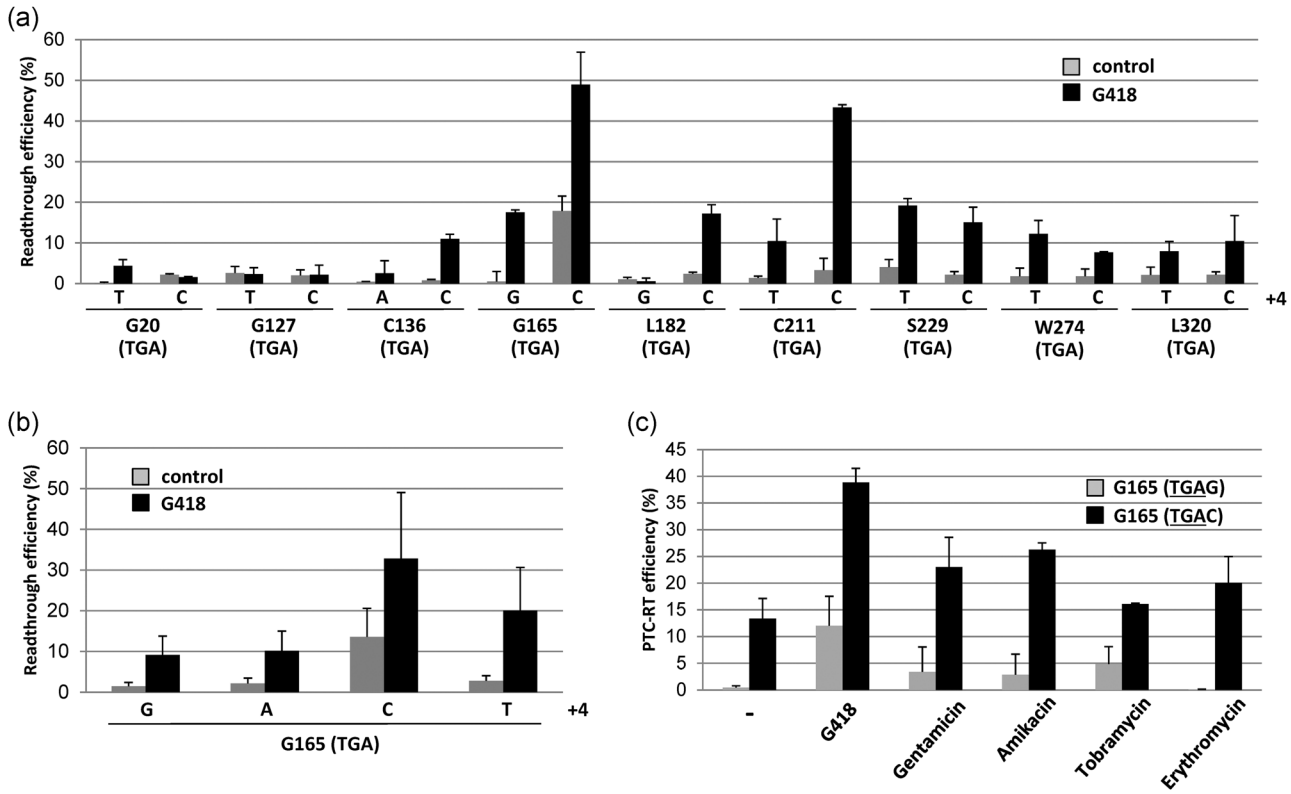

FIGURE 4 Influence of the proximal nucleotide sequence context on PTEN readthrough. (a) Influence of +4C nucleotide on different TGA PTC (premature termination codons). The readthrough of different TGA PTC in response to G418 (200 μg/ml) (left bars; the indicated nucleotide corresponds to the wild-type +4 nucleotide for each TGA) is compared with the readthrough of variants containing a C at position +4 (right bars), as indicated. See Table S1 for the recommended HGVS nomenclature for each mutation. (b) Influence of +4 nucleotide on G165X [p.(Gly165Ter)] TGA PTC. The readthrough of G165X TGA +4G/A/C/T PTC in response to G418 is shown. (c) Influence of +4C nucleotide upon distinct readthrough inducers. The readthrough of G165X TGA +4G/C in response to different readthrough inducers (concentrations are as in Figure 2h) is shown. Data are shown as the mean ± *SD* from at least two independent experiments, as in Figure 2h

which monitors the PTEN PIP3 phosphatase activity in cells (Cid et al., 2008; Rodriguez-Escudero et al., 2015). First, we performed experiments on the more likely PTEN variants obtained by readthrough from the more frequent *PTEN* PTC mutations. This is based on the reported incorporation frequency, for each PTC type, of specific amino acids during G418-induced readthrough in mammalian cells [TGA: Arg (R), 64.5% incorporation; Cys (C), 17.7%; Trp (W), 17.9%. TAG: Gln (Q), 86.5%; Tyr (Y), 10.8%; Lys (K), 2%. TAA: Gln (Q), 52%; Tyr (Y), 47.9%] (Roy et al., 2016). Figure 5 shows examples, using two different yeast functional assays, on the functional status of the potential PTEN variants generated by readthrough of PTC mutations R130X (TGA), R233X (TGA), R335X (TGA), S59X (TAA) [c.176C>A, p.(Ser59Ter)], and S59X (TGA) [c.176C>G, p.(Ser59Ter)]. As observed, all the R233, R335, and S59 experimental variants displayed functional activity similar to PTEN wild-type, with the exception of R335W, which displayed reduced functional activity. The R130 variants, as well as the R130X, R233X, and R335X PTC mutations, or the canonical catalytically inactive PTEN C124S mutation [c.371G>C, p.(Cys124Ser)], did not display any functional activity. For practical purposes, we define the functional activity of each PTEN amino acid substitution as its *functional score*, and we consider functional score values as 1 (functional activity similar to PTEN wild-type; for instance, R233C), 0.5 (functional activity reduced; for instance, R335W), or 0 (very low or absent functional activity; for instance, R130C) (Figure 5). Next, we extended our functional analysis to the bulk of PTEN potential variants generated by readthrough from the disease-associated PTEN PTCome. For this analysis, we retrieved PTEN variants functional performances from the high-throughput analysis using our yeast platform reported by Mighell et al. (2018), and we performed additional functional experiments on selected PTC-targeted PTEN residues or on those PTC positions from which functional data of the corresponding mutations were not available. The resulting functional scores for each potential PTEN variant resulting from readthrough of the disease-associated PTEN PTCome are summarized in Table S1 and information on the more frequent PTEN PTC is given in Table 2.

To provide predictive information on the readthrough functional reconstitution of the PTEN PTCome, we define *a readthrough efficiency score* for each PTC. This score considers the variables of the readthrough efficiency of each PTC as well as the functional score of the PTEN variants potentially generated by readthrough, adjusted by the amino acid incorporation frequency associated with each variant.

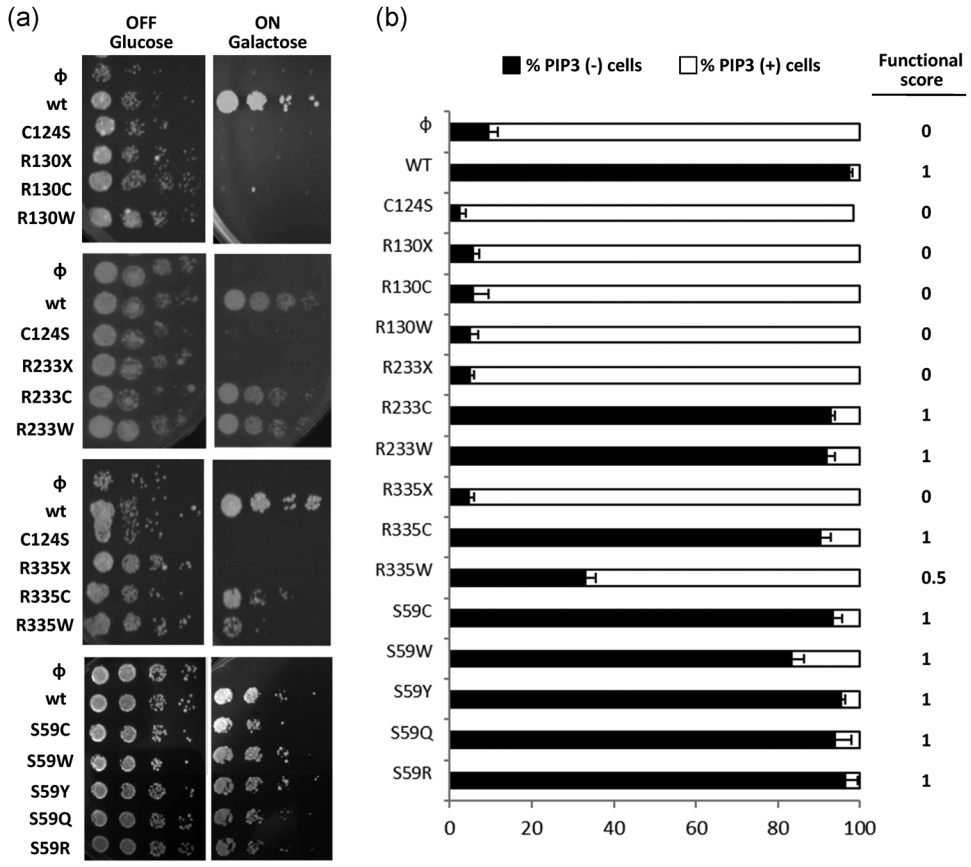

FIGURE 5 Functional analysis of PTEN mutations on PTEN PTC (premature termination codon)-targeted residues using a yeast heterologous system. (a) In vivo assessment of the catalytic function of PTEN readthrough variants by yeast drop growth assay. Yeast growth drop assays are shown of cells cotransformed with plasmids encoding the hyperactive p110α-CAAX form of the mammalian PI3K p110α catalytic subunit and PTEN variants, under glucose growth conditions (control, no induction of heterologous proteins) or galactose growth conditions (induction of heterologous proteins). The growth of yeast cells is inhibited by PI3K (Φ), and this can be prevented by the expression of active PTEN (wild-type [wt]) but not catalytically inactive PTEN mutations [C124S (Cys124Ser)]. Experiments are shown with PTEN variants mimicking the more likely residues incorporated by readthrough of the PTC R130X [p.(Arg130Ter)], R233X [p.(Arg233Ter)], R335X [p.(Arg335Ter)}, S59X TGA [p.(Ser59Ter)], and S59X TAA [p.(Ser59Ter)]. Experimental variants are as follows: R130C [c.388C>T, c390A>C, p.(Arg130Cys)], R130W [c.388C>T, c390A>G, p.(Arg130Trp)], R233C [c.697C>T, c.699A>C, p.(Arg233Cys)], R233W [c.697C>T, c.699A>G, p.(Arg233Trp)], R335C [c.1003C>T, c.1005A>T, p(Arg335Cys)], R335W [c.1003C>T, c.1005A>G, p(Arg335Trp)], S59R [c.175T>A, c.176C>G, p.(Ser59Arg)], S59C [c.176C>G, c.177A>C, p.(Ser59Cys)], S59W [c.176C>G, c.177A>G, p.(Ser59Trp)], S59Y [c.176C>A, c.177A>C, p.(Ser59Tyr)], and S59Q [c.175T>C, c.176C>A, p.(Ser59Gln)]. The catalytically inactive PTEN C124S mutation [c.371G>C, p.(Cys124Ser)] is also included. In all cases, one representative experiment is shown from at least two independent experiments. (b) In vivo quantitative assessment of the catalytic function of readthrough PTEN variants using a PIP3-sensor reporter. The activity of PTEN variants was quantified cotransforming the yeast with plasmids encoding a GFP-AKT1 reporter, which binds to PIP3 at the plasma membrane, followed by microscopical monitoring. Removal of the GFP-AKT1 reporter from the plasma membrane is a readout of PTEN PIP3-phosphatase activity. Data are the average of three experiments on three different clones ($n > 100$ cells per clone). Bars correspond to the standard deviation(±*SD*) and functional scores are provided (1, functional activity similar to PTEN wild-type; 0.5 functional activity reduced; 0, very low or absent functional activity)

This readthrough efficiency score ranges from 0 (0% of readthrough or functional score = 0) to the maximal of readthrough (maximal readthrough and functional score = 1), and a detailed definition of it is provided in Section 2. As shown, the readthrough efficiency score corrects the potential of PTEN functional reconstitution of some PTC undergoing optimal- or suboptimal-induced readthrough (Figure 3b and Tables S1 and 2), which is relevant for targeted-therapy patient segregation. For instance, the G129X PTC [c.385G>T, p.(Gly129Ter)] displayed suboptimal readthrough (14.4% readthrough efficiency), but functional score values = 0, resulting in readthrough efficiency score = 0. On the contrary, PTC such as S59X (TGA) or G230X displayed optimal readthrough and functional score = 1, rendering readthrough efficiency score equal to their readthrough efficiencies (28.9% and 28.1%, respectively). The high-frequency R130X, R233X, and R335X PTC displayed readthrough efficiency scores of 12.6, 25.2, and 15.5, respectively, indicating their suitability for readthrough reconstitution. The readthrough efficiency score could have informative utility in the potential implementation of readthrough-based therapies.

3.5 | Functional reconstitution of PTEN by translational readthrough

We have validated our scoring system directly assessing whether the induction of readthrough on some specific *PTEN* PTC mutations resulted in the reconstitution of a functional PTEN protein, as revealed by their effect on the phosphorylation status of coexpressed AKT on COS-7 mammalian cells and their ability to translocate to the nucleus. Selected PTEN PTC variants showing optimal or suboptimal readthrough efficiency and readthrough efficiency score above 10, including those with higher frequency in association with the disease (S59X [TGA], R130X, R233X, and R335X) displayed a functional activity upon G418 readthrough-induction comparable to the functional activity of PTEN wild-type, as monitored by p-AKT status. The *PTEN* PTC mutation Y176X (TAA) [c.528T>A, p.(Tyr176Ter)] not responding to induced readthrough (1.3% readthrough efficiency) and displaying a readthrough efficiency score = 1.3, did not show significant functional activity (Figure 6a,b). As PTEN cytoplasm/nucleus shuttling is important for PTEN function (Gil et al., 2007; Ho et al., 2020), we also tested in COS-7 cells the nuclear accumulation of PTEN PTC mutations upon readthrough induction. For these experiments, a PTEN-GFP Q17P variant [c.50A>C, p.(Gln17Pro)] which accumulates in the nucleus was used (Mingo et al., 2018). As shown in the Q17P background, the R130X and R233X mutations, but not the Y176 (TAA) mutation, were efficiently detected inside the nucleus upon readthrough induction (Figure 6c), in concordance with their detection as PTEN-GFP full-length proteins (Figure 6d). Together, our results indicate that inducible readthrough has the competence to reconstitute PTEN full-length functional proteins, both in terms of PIP3 phosphatase activity in cells and cytoplasm/nucleus dynamic shuttling. Interestingly, PTEN functional reconstitution was even achieved in the case of PTC targeting essential residues, such as the R130 catalytic residue, which is highly sensitive to loss-of-function by amino acid substitution (Rodriguez-Escudero et al., 2015). This can be explained by the relatively high frequency incorporation, upon readthrough of some PTC, of the wild-type amino acid (Roy et al., 2016; Xue et al., 2017).

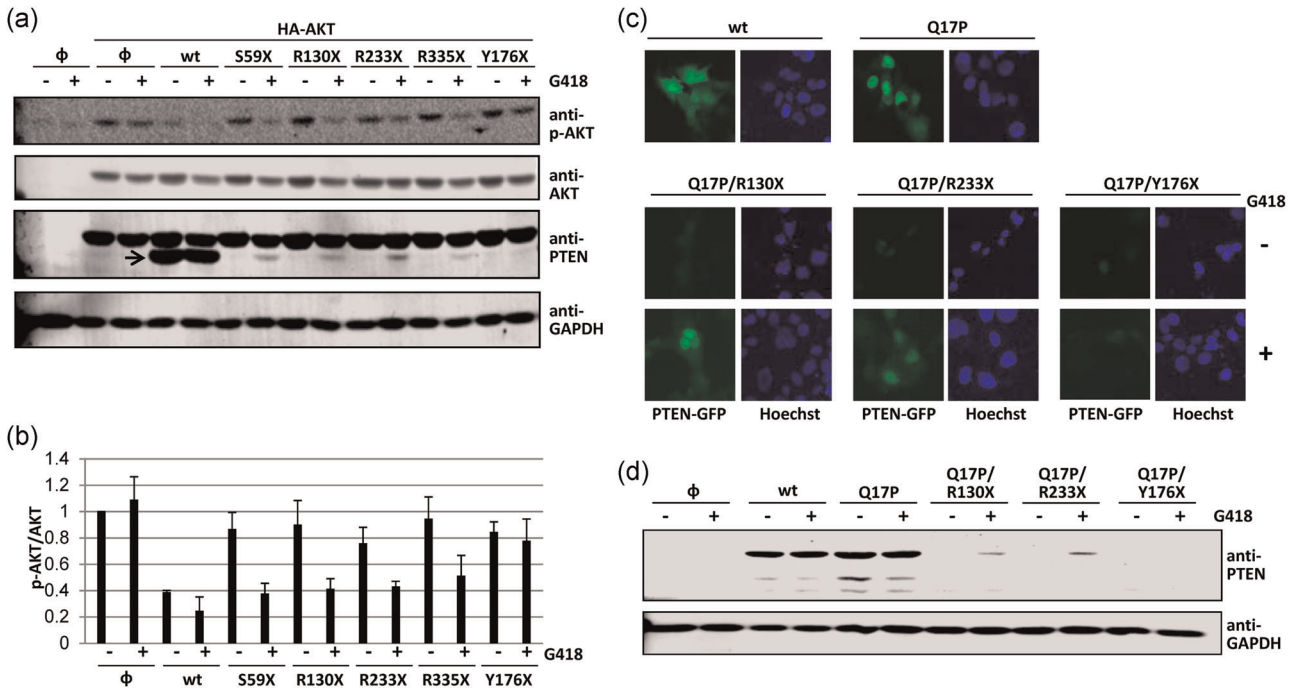

FIGURE 6 Functional reconstitution of PTEN mutations by readthrough. (a, b) Reconstitution of PTEN catalytic activity in cells. COS-7 cells were transfected with pRK5 plasmids containing the different PTEN variants, alone or in combination with the pSG5 HA-AKT plasmid, as indicated. Twenty-four hours posttransfection cells were kept untreated or incubated in the presence of G418 (200 μg/ml) for an additional 24 h, as indicated. HA-pAKT, HA-AKT, and PTEN proteins were detected by immunoblot using anti-pAKT or anti-AKT antibodies or the anti-PTEN 6H2.1 mAb. The arrow indicates the migration of PTEN. Detection of glyceraldehyde 3-phosphate dehydrogenase (GAPDH) with anti-GAPDH antibody is shown as a control. Ø, empty vector. In (a), a representative experiment is shown. In (b), quantification of the ratio pAKT/AKT is shown relative to PTEN wild-type (wt) untreated conditions (value = 1) (mean ± *SD* from two independent experiments), as determined by protein band quantification. (c, d) Reconstitution of PTEN nuclear accumulation. COS-7 cells were transfected with the different PTEN-GFP (C-terminal tagging) variants, and 24-h posttransfection cells were kept untreated or incubated in the presence of G418 (200 μg/ml) for an additional 24 h, as indicated. In (C), cells were directly processed for fluorescence microscopy. The upper panels show the localization of PTEN-GFP wild type and Q17P [p.(Gln17Pro)] in untreated cells. The lower panels show the localization of the different compound mutations in untreated and G418-treated cells. For each PTEN-GFP variant, the left panel shows PTEN-GFP localization (green), and the right panel shows the nuclei localization (blue), as stained with Hoechst. In (D), cells were processed for immunoblot analysis to monitor the readthrough-induced reconstitution of PTEN-GFP mutations, as in Figure 2a. In all cases, blots and pictures show one representative experiment from at least two independent experiments

In summary, using the tumor suppressor PTEN as a paradigm, we here define the collection of PTC mutations found in a gene in association with the disease as its disease-associated PTCome and set the basis to perform global translational and functional gene readthrough analysis of the PTCome from human disease-related genes. Our global expression analysis of the 141 variants of the disease-associated PTEN PTCome unveiled the existence of stable N- and C-terminal truncations generated from specific *PTEN* PTC mutations, which could be relevant in the interpretation of the PTEN functional phenotypes associated with patients carrying these mutations. In addition, our comprehensive readthrough comparative analysis, using the translation of the complete PTEN protein as the readout, confirms the importance of the PTC identity and its proximal nucleotide sequence context in the readthrough efficiency. This implies that utilization of effective gene mutation-specific readthrough-based therapies will require the precise experimental determination of the readthrough-response of the affected gene, as well as the monitoring of the functional properties of the readthrough-reconstituted proteins. We have defined a readthrough efficiency score taking into consideration these factors, which should be adjusted and validated for each different protein subjected to readthrough reconstitution. From our in vitro validation experiments, we hypothesize that in the case of PTEN, a readthrough efficiency score above 10 could predict potential benefit from PTEN functional restoration upon readthrough induction. Out of 30 PTC (21%) from the disease-associated PTEN PTCome displaying optimal or suboptimal readthrough, 22 PTC (16%) showed a readthrough efficiency score above 10 (Tables S1 and 2). The higher frequency PTEN PTC (R130X, R233X, and R335X) displayed high readthrough efficiency score and could be functionally reconstituted in cells upon readthrough, indicating that these PTEN mutations could potentially benefit from readthrough-based therapies. This approach could complement the efficacy of current therapeutic treatments indicated upon PTEN loss-of-function conditions, such as those based on PI3K/AKT/mTOR pathway inhibition. When addressing the therapeutic potential of the translational readthrough to reconstitute PTEN biological activity, it is important to take into consideration that *PTEN* is a haploinsufficient gene (Alimonti et al., 2010) and that a dominant-negative effect has been attributed to some PTEN variants associated with the disease (Papa et al., 2014). Additional evidence is required, in a more physiologic context, to verify the benefits of readthrough-mediated rescuing of PTEN functions. This includes the use of specific *Pten* knock-in mouse models, as well as heterozygous human cells displaying physiologic PTEN expression levels. Most of our comprehensive analysis has been made using G418 as a highly efficient readthrough inducer. As G418 is a toxic compound, the finding and characterization of optimal nontoxic readthrough inducers, alone or in combinations, is a necessity. We propose the use of the readthrough efficiency score as a general scoring system providing information on the potential benefit of low toxicity readthrough inducers for groups of patients carrying specific disease-associated PTC mutations. Gene- and protein-specific analyses of readthrough will be required to obtain readthrough efficiency scores that take into consideration the functional properties of the reconstituted protein as well as the readthrough inducer compound used. This will facilitate the rational segregation of readthrough-responder patients carrying specific PTC mutations, which will be determinant to optimize the potential benefits of readthrough-based precision therapies.

ACKNOWLEDGMENTS

We thank Gustavo Pérez-Nanclares and Ana Belén de la Hoz (Plataforma de Genética-Genómica, Biocruces Bizkaia Health Research Institute) for their expert assistance with DNA sequencing. This study was partially supported by grants SAF2016-79847-R (to Rafael Pulido and José I. López) and BIO2016-75030 (to Víctor J. Cid and María Molina) from Ministerio de Economía y Competitividad (Spain and Fondo Europeo de Desarrollo Regional), S2017/BMD-3691 (InGEMICS-CM) from Comunidad de Madrid and European Structural and Investment Funds (to Víctor J. Cid and María Molina), and grant 239813 from The Norwegian Research Council, Norway (to Caroline E. Nunes-Xavier). Janire Mingo and Asier Erramuzpe have been the recipients of a predoctoral fellowship (PRE_2014_1_285 to Janire Mingo and PRE_2014_1_252 to Asier Erramuzpe) from Gobierno Vasco, Departamento de Educación (Basque Country, Spain). Caroline E. Nunes-Xavier is the recipient of a Miguel Servet research contract from Instituto de Salud Carlos III (ISCIII, Spain) (CP20/00008). Leire Torices is the recipient of a predoctoral fellowship from Asociación Española Contra el Cáncer (AECC, Junta Provincial de Bizkaia, Spain).

CONFLICT OF INTERESTS

The authors declare that there are no conflict of interests.

DATA AVAILABILITY STATEMENT

The data that supports the findings of this study are available in the material of this article.

ORCID

Rafael Pulido http://orcid.org/0000-0001-9100-248X

REFERENCES

Alimonti, A., Carracedo, A., Clohessy, J. G., Trotman, L. C., Nardella, C., Egia, A., Salmena, L., Sampieri, K., Haveman, W. J., Brogi, E., Richardson, A. L., Zhang, J., & Pandolfi, P. P. (2010). Subtle variations in Pten dose determine cancer susceptibility. *Nature Genetics*, *42*(5), 454–458. https://doi.org/10.1038/ng.556

Alvarez-Garcia, V., Tawil, Y., Wise, H. M., & Leslie, N. R. (2019). Mechanisms of PTEN loss in cancer: It's all about diversity. *Seminars in Cancer Biology*, *59*, 66–79. https://doi.org/10.1016/j.semcancer.2019.02.001

Andrés-Pons, A., Rodríguez-Escudero, I., Gil, A., Blanco, A., Vega, A., Molina, M., Pulido, R., & Cid, V. J. (2007). In vivo functional analysis of the counterbalance of hyperactive phosphatidylinositol 3-kinase p110 catalytic oncoproteins by the tumor suppressor PTEN. *Cancer Research*, *67*(20), 9731–9739. https://doi.org/10.1158/0008-5472.CAN-07-1278

Asiful Islam, M., Alam, F., Kamal, M. A., Gan, S. H., Wong, K. K., & Sasongko, T. H. (2017). Therapeutic suppression of nonsense mutation: An emerging target in multiple diseases and thrombotic

disorders. *Current Pharmaceutical Design*, *23*(11), 1598–1609. https://doi.org/10.2174/1381612823666161122142950

Atkinson, J., & Martin, R. (1994). Mutations to nonsense codons in human genetic disease: Implications for gene therapy by nonsense suppressor tRNAs. *Nucleic Acids Research*, *22*(8), 1327–1334. https://doi.org/10.1093/nar/22.8.1327

Baradaran-Heravi, A., Balgi, A. D., Zimmerman, C., Choi, K., Shidmoossavee, F. S., Tan, J. S., Bergeaud, C., Krause, A., Flibotte, S., Shimizu, Y., Anderson, H. J., Mouly, V., Jan, E., Pfeifer, T., Jaquith, J. B., & Roberge, M. (2016). Novel small molecules potentiate premature termination codon readthrough by aminoglycosides. *Nucleic Acids Research*, *44*(14), 6583–6598. https://doi.org/10.1093/nar/gkw638

Bidou, L., Bugaud, O., Belakhov, V., Baasov, T., & Namy, O. (2017). Characterization of new-generation aminoglycoside promoting premature termination codon readthrough in cancer cells. *RNA Biology*, *14*(3), 378–388. https://doi.org/10.1080/15476286.2017.1285480

Bidou, L., Hatin, I., Perez, N., Allamand, V., Panthier, J. J., & Rousset, J. P. (2004). Premature stop codons involved in muscular dystrophies show a broad spectrum of readthrough efficiencies in response to gentamicin treatment. *Gene Therapy*, *11*(7), 619–627. https://doi.org/10.1038/sj.gt.3302211

Bubien, V., Bonnet, F., Brouste, V., Hoppe, S., Barouk-Simonet, E., David, A., Edery, P., Bottani, A., Layet, V., Caron, O., Gilbert-Dussardier, B., Delnatte, C., Dugast, C., Fricker, J. P., Bonneau, D., Sevenet, N., Longy, M., & Caux, F. (2013). High cumulative risks of cancer in patients with PTEN hamartoma tumour syndrome. *Journal of Medical Genetics*, *50*(4), 255–263. https://doi.org/10.1136/jmedgenet-2012-101339

Campofelice, A., Lentini, L., Di Leonardo, A., Melfi, R., Tutone, M., Pace, A., & Pibiri, I. (2019). Strategies against Nonsense: Oxadiazoles as translational readthrough-inducing drugs (TRIDs). *International Journal of Molecular Sciences*, *20*(13), 3329. https://doi.org/10.3390/ijms20133329

Cid, V. J., Rodríguez-Escudero, I., Andrés-Pons, A., Romá-Mateo, C., Gil, A., den Hertog, J., Molina, M., & Pulido, R. (2008). Assessment of PTEN tumor suppressor activity in nonmammalian models: The year of the yeast. *Oncogene*, *27*(41), 5431–5442. https://doi.org/10.1038/onc.2008.240

Cohen, S., Kramarski, L., Levi, S., Deshe, N., Ben David, O., & Arbely, E. (2019). Nonsense mutation-dependent reinitiation of translation in mammalian cells. *Nucleic Acids Research*, *47*(12), 6330–6338. https://doi.org/10.1093/nar/gkz319

Dabrowski, M., Bukowy-Bieryllo, Z., & Zietkiewicz, E. (2015). Translational readthrough potential of natural termination codons in eucaryotes—The impact of RNA sequence. *RNA Biology*, *12*(9), 950–958. https://doi.org/10.1080/15476286.2015.1068497

Dabrowski, M., Bukowy-Bieryllo, Z., & Zietkiewicz, E. (2018). Advances in therapeutic use of a drug-stimulated translational readthrough of premature termination codons. *Molecular Medicine*, *24*(1), 25. https://doi.org/10.1186/s10020-018-0024-7

Floquet, C., Deforges, J., Rousset, J. P., & Bidou, L. (2011). Rescue of non-sense mutated p53 tumor suppressor gene by aminoglycosides. *Nucleic Acids Research*, *39*(8), 3350–3362. https://doi.org/10.1093/nar/gkq1277

Floquet, C., Hatin, I., Rousset, J. P., & Bidou, L. (2012). Statistical analysis of readthrough levels for nonsense mutations in mammalian cells reveals a major determinant of response to gentamicin. *PLOS Genetics*, *8*(3), e1002608. https://doi.org/10.1371/journal.pgen.1002608

Floquet, C., Rousset, J. P., & Bidou, L. (2011). Readthrough of premature termination codons in the adenomatous polyposis coli gene restores its biological activity in human cancer cells. *PLOS One*, *6*(8), e24125. https://doi.org/10.1371/journal.pone.0024125

Friesen, W. J., Trotta, C. R., Tomizawa, Y., Zhuo, J., Johnson, B., Sierra, J., Roy, B., Weetall, M., Hedrick, J., Sheedy, J., Takasugi, J., Moon, Y. C., Babu, S., Baiazitov, R., Leszyk, J. D., Davis, T. W., Colacino, J. M., Peltz, S. W., & Welch, E. M. (2017). The nucleoside analog clitocine is a potent and efficacious readthrough agent. *RNA*, *23*(4), 567–577. https://doi.org/10.1261/rna.060236.116

Georgescu, M. M., Kirsch, K. H., Akagi, T., Shishido, T., & Hanafusa, H. (1999). The tumor-suppressor activity of PTEN is regulated by its carboxyl-terminal region. *Proceedings of the National Academy of Sciences of the United States of America*, *96*(18), 10182–10187.

Georgescu, M. M., Kirsch, K. H., Kaloudis, P., Yang, H., Pavletich, N. P., & Hanafusa, H. (2000). Stabilization and productive positioning roles of the C2 domain of PTEN tumor suppressor. *Cancer Research*, *60*(24), 7033–7038.

Gil, A., Andrés-Pons, A., Fernández, E., Valiente, M., Torres, J., Cervera, J., & Pulido, R. (2006). Nuclear localization of PTEN by a Ran-dependent mechanism enhances apoptosis: Involvement of an N-terminal nuclear localization domain and multiple nuclear exclusion motifs. *Molecular Biology of the Cell*, *17*(9), 4002–4013. https://doi.org/10.1091/mbc.E06-05-0380

Gil, A., Andrés-Pons, A., & Pulido, R. (2007). Nuclear PTEN: A tale of many tails. *Cell Death and Differentiation*, *14*(3), 395–399. https://doi.org/10.1038/sj.cdd.4402073

Gil, A., Lopez, J. I., & Pulido, R. (2016). Assessing PTEN subcellular localization. *Methods in Molecular Biology*, *1388*, 169–186. https://doi.org/10.1007/978-1-4939-3299-3_12

Han, S. Y., Kato, H., Kato, S., Suzuki, T., Shibata, H., Ishii, S., & Ishioka, C. (2000). Functional evaluation of PTEN missense mutations using in vitro phosphoinositide phosphatase assay. *Cancer Research*, *60*(12), 3147–3151.

Hermann, T. (2007). Aminoglycoside antibiotics: Old drugs and new therapeutic approaches. *Cellular and Molecular Life Science*, *64*(14), 1841–1852. https://doi.org/10.1007/s00018-007-7034-x

Ho, J., Cruise, E. S., Dowling, R. J. O., & Stambolic, V. (2020). PTEN nuclear functions. *Cold Spring Harbor Perspectives in Medicine*, *10*(5), a036079. https://doi.org/10.1101/cshperspect.a036079

Howard, M. T., Shirts, B. H., Petros, L. M., Flanigan, K. M., Gesteland, R. F., & Atkins, J. F. (2000). Sequence specificity of aminoglycoside-induced stop condon readthrough: Potential implications for treatment of Duchenne muscular dystrophy. *Annals of Neurology*, *48*(2), 164–169.

Keeling, K. M., & Bedwell, D. M. (2002). Clinically relevant aminoglycosides can suppress disease-associated premature stop mutations in the IDUA and P53 cDNAs in a mammalian translation system. *Journal of Molecular Medicine (Berlin)*, *80*(6), 367–376. https://doi.org/10.1007/s00109-001-0317-z

Keeling, K. M., Xue, X., Gunn, G., & Bedwell, D. M. (2014). Therapeutics based on stop codon readthrough. *Annual Review of Genomics and Human Genetics*, *15*, 371–394. https://doi.org/10.1146/annurev-genom-091212-153527

Lee, Y. R., Chen, M., & Pandolfi, P. P. (2018). The functions and regulation of the PTEN tumour suppressor: New modes and prospects. *Nature Reviews Molecular Cell Biology*, *19*(9), 547–562. https://doi.org/10.1038/s41580-018-0015-0

Leslie, N. R., & Foti, M. (2011). Non-genomic loss of PTEN function in cancer: Not in my genes. *Trends In Pharmacological Sciences*, *32*(3), 131–140. https://doi.org/10.1016/j.tips.2010.12.005

Liang, F., Shang, H., Jordan, N. J., Wong, E., Mercadante, D., Saltz, J., & Mense, M. (2017). High-throughput screening for readthrough modulators of CFTR PTC mutations. *SLAS Technology*, *22*(3), 315–324. https://doi.org/10.1177/2472630317692561

Linde, L., & Kerem, B. (2008). Introducing sense into nonsense in treatments of human genetic diseases. *Trends in Genetics*, *24*(11), 552–563. https://doi.org/10.1016/j.tig.2008.08.010

Luna, S., Mingo, J., Aurtenetxe, O., Blanco, L., Amo, L., Schepens, J., Hendriks, W. J., & Pulido, R. (2016). Tailor-made protein tyrosine phosphatases: In vitro site-directed mutagenesis of PTEN and PTPRZ-B. *Methods in Molecular Biology*, *1447*, 79–93. https://doi.org/10.1007/978-1-4939-3746-2_5

Manuvakhova, M., Keeling, K., & Bedwell, D. M. (2000). Aminoglycoside antibiotics mediate context-dependent suppression of termination codons in a mammalian translation system. *RNA*, *6*(7), 1044–1055. https://doi.org/10.1017/s1355838200000716

Midgley, J. (2019). A breakthrough in readthrough? Could geneticin lead the way to effective treatment for cystinosis nonsense mutations? *Pediatric Nephrology*, *34*(5), 917–920. https://doi.org/10.1007/s00467-018-4173-2

Mighell, T. L., Evans-Dutson, S., & O'Roak, B. J. (2018). A saturation mutagenesis approach to understanding PTEN lipid phosphatase activity and genotype-phenotype relationships. *American Journal of Human Genetics*, *102*(5), 943–955. https://doi.org/10.1016/j.ajhg.2018.03.018

Milella, M., Falcone, I., Conciatori, F., Cesta Incani, U., Del Curatolo, A., Inzerilli, N., Nuzzo, C. M. A., Vaccaro, V., Vari, S., Cognetti, F., & Ciuffreda, L. (2015). PTEN: Multiple functions in human malignant tumors. *Frontiers in Oncology*, *5*, 24. https://doi.org/10.3389/fonc.2015.00024

Mingo, J., Erramuzpe, A., Luna, S., Aurtenetxe, O., Amo, L., Diez, I., Schepens, J. T. G., Hendriks, W. J. A. J., Cortés, J. M., & Pulido, R. (2016). One-tube-only standardized site-directed mutagenesis: An alternative approach to generate amino acid substitution collections. *PLOS One*, *11*(8), e0160972. https://doi.org/10.1371/journal.pone.0160972

Mingo, J., Luna, S., Gaafar, A., Nunes-Xavier, C. E., Torices, L., Mosteiro, L., Ruiz, R., Guerra, I., Llarena, R., Angulo, J. C., López, J. I., & Pulido, R. (2019). Precise definition of PTEN C-terminal epitopes and its implications in clinical oncology. *NPJ Precision Oncology*, *3*, 11. https://doi.org/10.1038/s41698-019-0083-4

Mingo, J., Rodríguez-Escudero, I., Luna, S., Fernández-Acero, T., Amo, L., Jonasson, A. R., Zori, R. T., López, J. I., Molina, M., Cid, V. J., & Pulido, R. (2018). A pathogenic role for germline PTEN variants which accumulate into the nucleus. *European Journal of Human Genetics*, *26*(8), 1180–1187. https://doi.org/10.1038/s41431-018-0155-x

Morais, P., Adachi, H., & Yu, Y. T. (2020). Suppression of nonsense mutations by new emerging technologies. *International Journal of Molecular Sciences*, *21*(12), 4394. https://doi.org/10.3390/ijms21124394

Mort, M., Ivanov, D., Cooper, D. N., & Chuzhanova, N. A. (2008). A meta-analysis of nonsense mutations causing human genetic disease. *Human Mutation*, *29*(8), 1037–1047. https://doi.org/10.1002/humu.20763

Nagel-Wolfrum, K., Moller, F., Penner, I., Baasov, T., & Wolfrum, U. (2016). Targeting nonsense mutations in diseases with translational read-through-inducing drugs (TRIDs). *BioDrugs*, *30*(2), 49–74. https://doi.org/10.1007/s40259-016-0157-6

Ngeow, J., & Eng, C. (2020). PTEN in hereditary and sporadic cancer. *Cold Spring Harbor Perspectives in Medicine*, *10*(4), a036087. https://doi.org/10.1101/cshperspect.a036087

Papa, A., Wan, L., Bonora, M., Salmena, L., Song, M. S., Hobbs, R. M., Lunardi, A., Webster, K., Ng, C., Newton, R. H., Knoblauch, N., Guarnerio, J., Ito, K., Turka, L. A., Beck, A. H., Pinton, P., Bronson, R. T., Wei, W., & Pandolfi, P. P. (2014). Cancer-associated PTEN mutants act in a dominant-negative manner to suppress PTEN protein function. *Cell*, *157*(3), 595–610. https://doi.org/10.1016/j.cell.2014.03.027

Peltz, S. W., Morsy, M., Welch, E. M., & Jacobson, A. (2013). Ataluren as an agent for therapeutic nonsense suppression. *Annual Review of Medicine*, *64*, 407–425. https://doi.org/10.1146/annurev-med-120611-144851

Pilarski, R., Stephens, J. A., Noss, R., Fisher, J. L., & Prior, T. W. (2011). Predicting PTEN mutations: An evaluation of Cowden syndrome and Bannayan-Riley-Ruvalcaba syndrome clinical features. *Journal of Medical Genetics*, *48*(8), 505–512. https://doi.org/10.1136/jmg.2011.088807

Pulido, R. (2015). PTEN: a yin-yang master regulator protein in health and disease. *Methods*, *77-78*, 3–10. https://doi.org/10.1016/j.ymeth.2015.02.009

Pulido, R., Mingo, J., Gaafar, A., Nunes-Xavier, C. E., Luna, S., Torices, L., Angulo, J. C., & López, J. I. (2019). Precise Immunodetection of PTEN protein in human neoplasia. *Cold Spring Harbor Perspectives in Medicine*, *9*(12), a036293. https://doi.org/10.1101/cshperspect.a036293

Rodriguez-Escudero, I., Fernandez-Acero, T., Bravo, I., Leslie, N. R., Pulido, R., Molina, M., & Cid, V. J. (2015). Yeast-based methods to assess PTEN phosphoinositide phosphatase activity in vivo. *Methods*, *77–78*, 172–179. https://doi.org/10.1016/j.ymeth.2014.10.020

Rodríguez-Escudero, I., Oliver, M. D., Andrés-Pons, A., Molina, M., Cid, V. J., & Pulido, R. (2011). A comprehensive functional analysis of PTEN mutations: Implications in tumor- and autism-related syndromes. *Human Molecular Genetics*, *20*(21), 4132–4142. https://doi.org/10.1093/hmg/ddr337

Rodríguez-Escudero, I., Roelants, F. M., Thorner, J., Nombela, C., Molina, M., & Cid, V. J. (2005). Reconstitution of the mammalian PI3K/PTEN/Akt pathway in yeast. *Biochemical Journal*, *390*(Pt 2), 613–623. https://doi.org/10.1042/BJ20050574

Roy, B., Friesen, W. J., Tomizawa, Y., Leszyk, J. D., Zhuo, J., Johnson, B., Dakka, J., Trotta, C. R., Xue, X., Mutyam, V., Keeling, K. M., Mobley, J. A., Rowe, S. M., Bedwell, D. M., Welch, E. M., & Jacobson, A. (2016). Ataluren stimulates ribosomal selection of near-cognate tRNAs to promote nonsense suppression. *Proceedings of the National Academy of Sciences of the United States of America*, *113*(44), 12508–12513. https://doi.org/10.1073/pnas.1605336113

Sabbavarapu, N. M., Shavit, M., Degani, Y., Smolkin, B., Belakhov, V., & Baasov, T. (2016). Design of novel aminoglycoside derivatives with enhanced suppression of diseases-causing nonsense mutations. *ACS Medicinal Chemistry Letters*, *7*(4), 418–423. https://doi.org/10.1021/acsmedchemlett.6b00006

Song, M. S., Salmena, L., & Pandolfi, P. P. (2012). The functions and regulation of the PTEN tumour suppressor. *Nature Reviews Molecular Cell Biology*, *13*(5), 283–296. https://doi.org/10.1038/nrm3330

Sotelo, N. S., Schepens, J. T., Valiente, M., Hendriks, W. J., & Pulido, R. (2015). PTEN-PDZ domain interactions: binding of PTEN to PDZ domains of PTPN13. *Methods*, *77-78*, 147–156. https://doi.org/10.1016/j.ymeth.2014.10.017

Spinelli, L., Black, F. M., Berg, J. N., Eickholt, B. J., & Leslie, N. R. (2015). Functionally distinct groups of inherited PTEN mutations in autism and tumour syndromes. *Journal of Medical Genetics*, *52*(2), 128–134. https://doi.org/10.1136/jmedgenet-2014-102803

Stenson, P. D., Mort, M., Ball, E. V., Evans, K., Hayden, M., Heywood, S., Hussain, M., Phillips, A. D., & Cooper, D. N. (2017). The Human Gene Mutation Database: Towards a comprehensive repository of inherited mutation data for medical research, genetic diagnosis and next-generation sequencing studies. *Human Genetics*, *136*(6), 665–677. https://doi.org/10.1007/s00439-017-1779-6

Tan, H., Bao, J., & Zhou, X. (2015). Genome-wide mutational spectra analysis reveals significant cancer-specific heterogeneity. *Scientific Reports*, *5*, 12566. https://doi.org/10.1038/srep12566

Tan, M. H., Mester, J., Peterson, C., Yang, Y., Chen, J. L., Rybicki, L. A., Milas, K., Pederson, H., Remzi, B., Orloff, M. S., & Eng, C. (2011). A clinical scoring system for selection of patients for PTEN mutation testing is proposed on the basis of a prospective study of 3042

probands. *American Journal of Human Genetics*, *88*(1), 42–56. https://doi.org/10.1016/j.ajhg.2010.11.013

Tate, J. G., Bamford, S., Jubb, H. C., Sondka, Z., Beare, D. M., Bindal, N., Boutselakis, H., Cole, C. G., Creatore, C., Dawson, E., Fish, P., Harsha, B., Hathaway, C., Jupe, S. C., Kok, C. Y., Noble, K., Ponting, L., Ramshaw, C. C., Rye, C. E., … Forbes, S. A. (2019). COSMIC: The Catalogue Of Somatic Mutations In Cancer. *Nucleic Acids Research*, *47*(D1), D941–D947. https://doi.org/10.1093/nar/gky1015

Tork, S., Hatin, I., Rousset, J. P., & Fabret, C. (2004). The major 5' determinant in stop codon read-through involves two adjacent adenines. *Nucleic Acids Research*, *32*(2), 415–421. https://doi.org/10.1093/nar/gkh201

Vazquez, F., Ramaswamy, S., Nakamura, N., & Sellers, W. R. (2000). Phosphorylation of the PTEN tail regulates protein stability and function. *Molecular and Cellular Biology*, *20*(14), 5010–5018.

Worby, C. A., & Dixon, J. E. (2014). Pten. *Annual Review of Biochemistry*, *83*, 641–669. https://doi.org/10.1146/annurev-biochem-082411-113907

Wright, G. D., & Thompson, P. R. (1999). Aminoglycoside phosphotransferases: Proteins, structure, and mechanism. *Frontiers in Bioscience*, *4*, D9–D21.

Xue, X., Mutyam, V., Thakerar, A., Mobley, J., Bridges, R. J., Rowe, S. M., Keeling, K. M., & Bedwell, D. M. (2017). Identification of the amino acids inserted during suppression of CFTR nonsense mutations and determination of their functional consequences. *Human Molecular Genetics*, *26*(16), 3116–3129. https://doi.org/10.1093/hmg/ddx196

Yehia, L., Keel, E., & Eng, C. (2020). The clinical spectrum of PTEN mutations. *Annual Review of Medicine*, *71*, 103–116. https://doi.org/10.1146/annurev-med-052218-125823

Zilberberg, A., Lahav, L., & Rosin-Arbesfeld, R. (2010). Restoration of APC gene function in colorectal cancer cells by aminoglycoside- and macrolide-induced read-through of premature termination codons. *Gut*, *59*(4), 496–507. https://doi.org/10.1136/gut.2008.169805

SUPPORTING INFORMATION

Additional Supporting Information may be found online in the supporting information tab for this article.

How to cite this article: Luna, S., Torices, L., Mingo, J., Amo, L., Rodríguez-Escudero, I., Ruiz-Ibarlucea, P., Erramuzpe, A., Cortés, J. M., Tejada, M. I., Molina, M., Nunes-Xavier, C. E., López, J. I., Cid, V. J., & Pulido, R. (2021). A global analysis of the reconstitution of PTEN function by translational readthrough of *PTEN* pathogenic premature termination codons. *Human Mutation*, 42, 551–566. https://doi.org/10.1002/humu.24186